LA-UR-14-26449

Title: Generic Crystalline Disposal Reference Case

Author(s): Painter, Scott Leroy
Chu, Shaoping
Harp, Dylan Robert
Perry, Frank Vinton
Wang, Yifeng

Intended for: Report

Issued: 2015-02-20 (rev.1)

GENERIC CRYSTALLINE DISPOSAL REFERENCE CASE

Fuel Cycle Research & Development

Prepared for
U.S. Department of Energy
Used Fuel Disposition Campaign
Scott L Painter, Shaoping Chu, Dylan Harp, Frank V Perry
Los Alamos National Laboratory
and
Yifeng Wang
Sandia National Laboratory

August 2014
FCRD-UFD-2014-00500
LA-UR-14-26449

Appendix E
FCT Document Cover Sheet

Name/Title of Deliverable/Milestone	Generic Crystalline Disposal Reference Case
Work Package Title and Number	Generic Natural Systems Evaluation - LANL
Work Package WBS Number	FT-14LA080801
Responsible Work Package Manager	Scott Painter
	(Name/Signature)

Date Submitted 8/15/2014

Quality Rigor Level for Deliverable/Milestone	☐ QRL-3	☐ QRL-2	☐ QRL-1 ☐ Nuclear Data	☒ N/A*

This deliverable was prepared in accordance with Los Alamos National Laboratory
(Participant/National Laboratory Name)

QA program which meets the requirements of

☒ DOE Order 414.1 ☐ NQA-1-2000

This Deliverable was subjected to:

☐ Technical Review

Technical Review (TR)

Review Documentation Provided

☐ Signed TR Report or,

☐ Signed TR Concurrence Sheet or,

☐ Signature of TR Reviewer(s) below

Name and Signature of Reviewers

☐ Peer Review

Peer Review (PR)

Review Documentation Provided

☐ Signed PR Report or,

☐ Signed PR Concurrence Sheet or,

☐ Signature of PR Reviewer(s) below

*Note: In some cases there may be a milestone where an item is being fabricated, maintenance is being performed on a facility, or a document is being issued through a formal document control process where it specifically calls out a formal review of the document. In these cases, documentation (e.g., inspection report, maintenance request, work planning package documentation or the documented review of the issued document through the document control process) of the completion of the activity along with the Document Cover Sheet is sufficient to demonstrate achieving the milestone. QRL for such milestones may be also be marked N/A in the work package provided the work package clearly specifies the requirement to use the Document Cover Sheet and provide supporting documentation.

EXECUTIVE SUMMARY

A generic reference case for disposal of spent nuclear fuel and high-level radioactive waste in crystalline rock is outlined. The generic cases are intended to support development of disposal system modeling capability by establishing relevant baseline conditions and parameters. Establishment of a generic reference case requires that the emplacement concept, waste inventory, waste form, waste package, backfill/buffer properties, EBS failure scenarios, host rock properties, and biosphere be specified. The focus in this report is on those elements that are unique to crystalline disposal, especially the geosphere representation.

Three emplacement concepts are suggested for further analyses: a waste packages containing 4 PWR assemblies emplaced in boreholes in the floors of tunnels (KBS-3 concept), a 12-assembly waste package emplaced in tunnels, and a 32-assembly dual purpose canister emplaced in tunnels. In addition, three failure scenarios were suggested for future use: a nominal scenario involving corrosion of the waste package in the tunnel emplacement concepts, a manufacturing defect scenario applicable to the KBS-3 concept, and a disruptive glaciation scenario applicable to both emplacement concepts.

The computational approaches required to analyze EBS failure and transport processes in a crystalline rock repository are similar to those of argillite/shale, with the most significant difference being that the EBS in a crystalline rock repository will likely experience highly heterogeneous flow rates, which should be represented in the model. The computational approaches required to analyze radionuclide transport in the natural system are very different because of the highly channelized nature of fracture flow. Computational workflows tailored to crystalline rock based on discrete transport pathways extracted from discrete fracture network models are recommended.

CONTENTS

FIGURES

TABLES

REFERENCE CASE FOR GENERIC CRYSTALLINE DISPOSAL SYSTEM

1. INTRODUCTION

The Used Fuel Disposition Campaign (UFDC) of the U.S. Department of Energy (DOE) Office of Nuclear Energy (NE) is conducting research and development (R&D) on generic deep geologic disposal systems for high-activity nuclear wastes, including existing waste and waste that is expected to be generated under future fuel cycles. The term high-activity waste refers collectively to both used nuclear fuel (UNF) from nuclear reactors and high-level radioactive waste (HLW) from reprocessing of UNF, and from other sources.

Disposal system modeling activities within UFDC are developing the necessary capability to perform generic disposal system simulations for salt, crystalline rock, clay/shale, and deep borehole disposal options, with a focus on more realistic process-based modeling. The Generic Safety Case provides preliminary evaluations of the safety of potential geologic disposal facilities, geologic media, and disposal technologies that might be evaluated in the future. Defining reference cases is a key step in developing a generic safety case. This report addresses the reference case for granite and other crystalline rocks.

Several countries have studied spent fuel disposal in crystalline rock. In particular, Sweden and Finland have performed detailed site investigation and safety assessment studies and have each submitted to the relevant regulatory authority an application for a license to construct a final repository. In addition, Canada, Japan and the US have operated underground research laboratories in granite.

Mariner et al. (2011) summarize some of the technical issues associated with disposal of high-activity waste in crystalline rock. The current report focuses on describing a small number of reference cases and scenarios for use in generic disposal system modeling.

2. GENERIC EMPLACEMENT CONCEPTS

Definition of a reference case requires that an emplacement concept be specified. The KBS-3 concept (SKB, 2011) developed in Sweden is arguably the disposal system concept at the most advanced stage of development for any medium. As developed, the KBS-3 concept is tailored for relatively small waste inventories (12,000 metric tons of heavy metal for the proposed Forsmark repository in Sweden and smaller inventories in Finland). Other emplacement concepts may be suitable for crystalline rock, including axial emplacements in tunnels, emplacement in massive cavities with our without a hydraulic cage to divert water, and mined repositories with borehole arrays. However, those alternative concepts have not been explored in any detail for crystalline rock.

The KBS-3 concept and axial emplacement in tunnels were chosen for further consideration. The KBS-3 concept is chosen for a reference case because it has been studied extensively. Emplacement in tunnels is chosen to maintain consistency with salt (Freeze et al., 2013) and argillite/shale (Zheng et al., 2014) reference cases.

2.1 Emplacement in tunnel boreholes

In the KBS-3 concept (Figure 2-1), boreholes are drilled in the bottom (KBS-3V concept) or side (KBS-3H concept) of repository tunnels. Waste containers are copper shells with cast iron inserts for structural integrity. Bentonite buffer material is to be placed between the canisters and the borehole wall. The relatively small diameter (~1 m) canisters contain 4 PWR assemblies in the existing KBS-3 concept.

2.2 Tunnel emplacement

An alternative to the KBS-3 concept, which would accommodate a larger number of PWR or BWR assemblies per canister, is direct emplacement in tunnels (Figures 2-2 to 2-4). Variants of this reference case include two types of waste package: a dual-purpose canister (DPC) that contains 32 PWR (Pressurized Water Reactor) fuel assemblies (Hardin et al., 2013) and canister that contains the inventory of 12 PWR assemblies (Freeze et al., 2013).

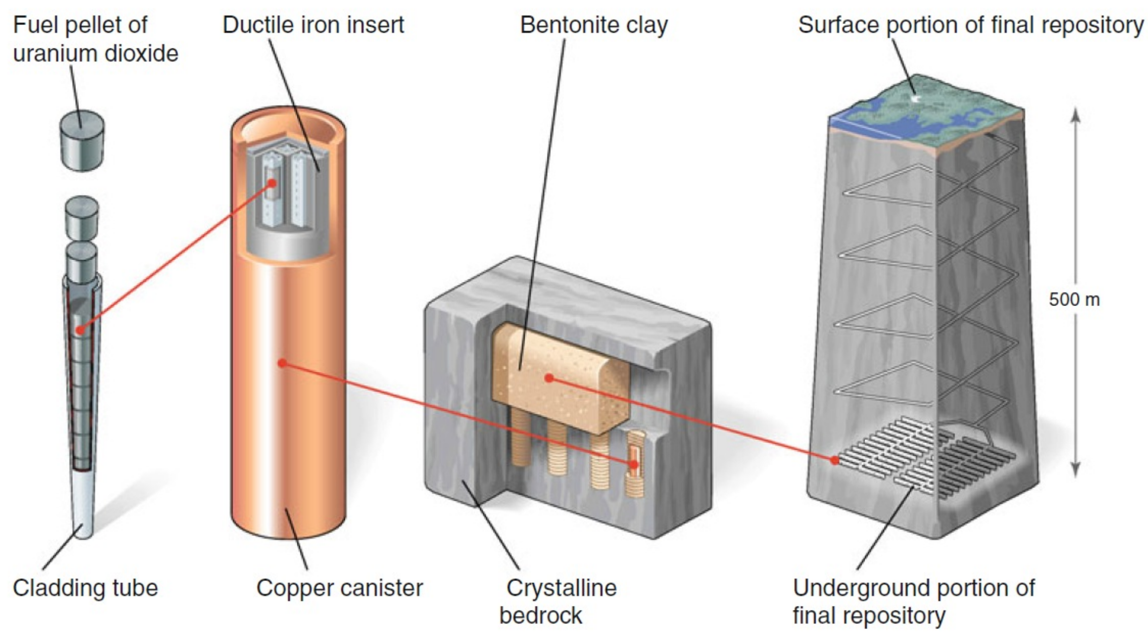

Figure 2-1. The KBS-3 Concept (SKB, 2011).

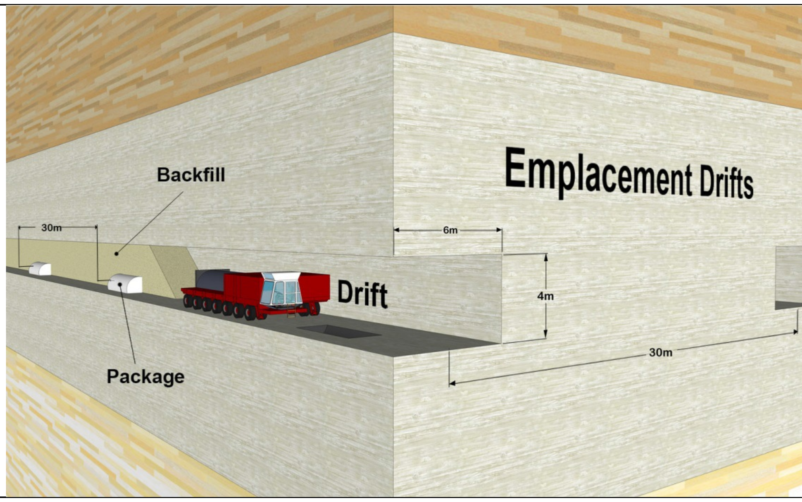

Figure 2-2. Emplacement in drifts with backfill.

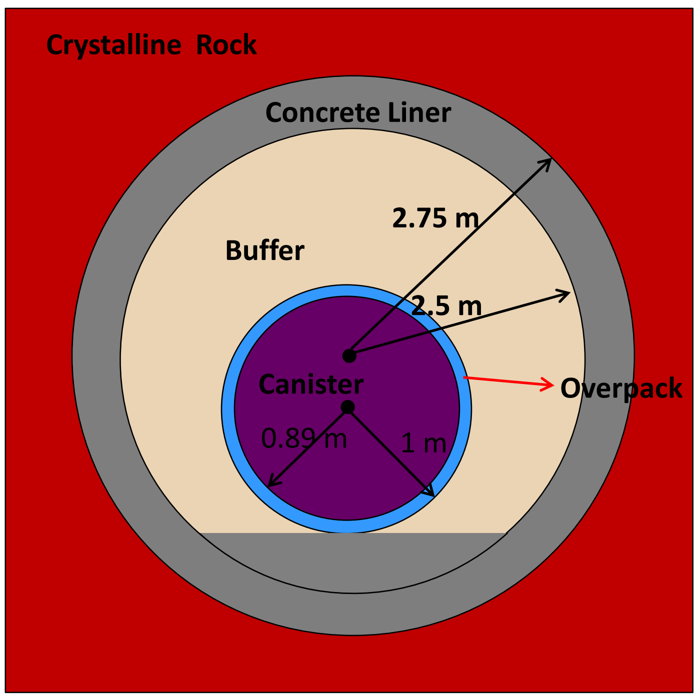

Figure 2-3. Geometry of a cross section of a drift for the disposal of DPC.

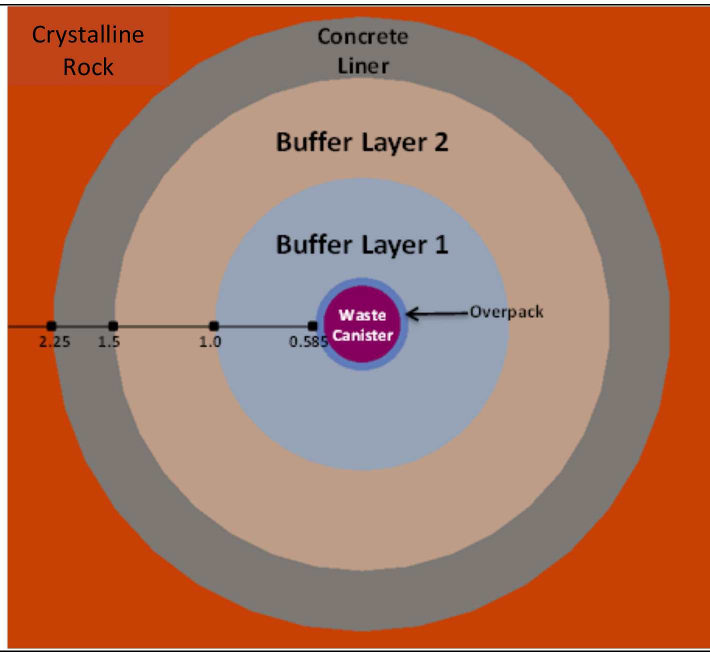

Figure 2-4. Schematic view of 2-D diagram of a double layer two-clay buffer layer EBS. Point values are radial distances in meters from the center of the waste canister (modified from Jove Colon et al. 2013).

3. ENGINEERED BARRIER SYSTEM

The description of the reference case EBS includes waste form, waste package, buffer/backfill, and seals. Common features with the argillite/shale reference case (Zheng et al. 2014) include the entire EBS concept for tunnel emplacement, as well as waste form, buffer properties, and seals in the KBS-3 concept. The common elements are not repeated here.

Waste packages in the KBS-3 concept (Figure 3-1) are described in detail in SKB reports (e.g. SKB, 2011, and references cited therein). The waste packages consist of a 5-cm copper shell with nodular cast iron inserts for structural integrity. Each canister contains approximately 7,400 kg of copper and 13,600 kg of cast iron (SKB, 2011).

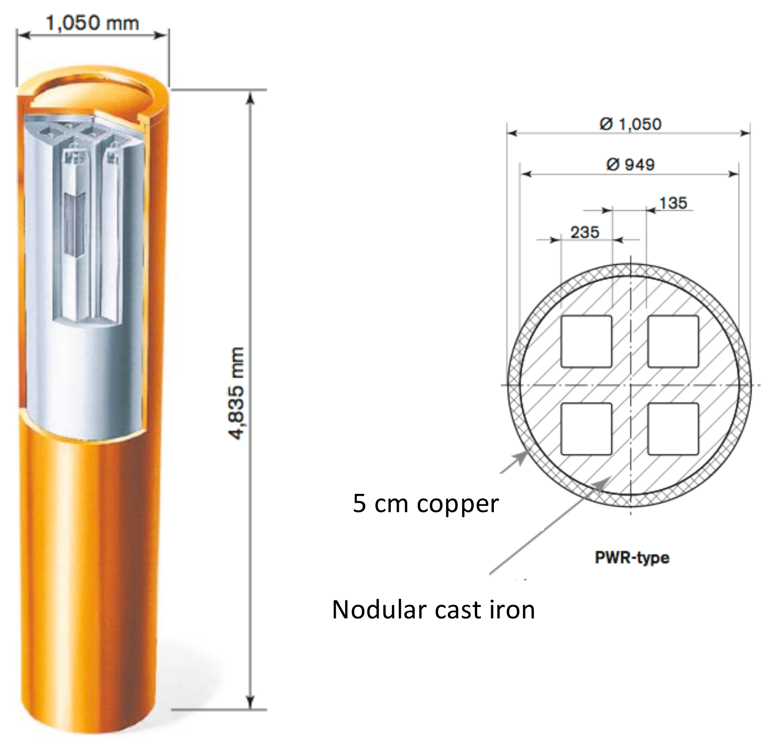

Figure 3-1. Waste package in the KBS-3 emplacement concept, assuming 4 PWR assemblies. Modified from SKB (2011).

4. NATURAL SYSTEM

Crystalline rocks are found in several distinct geologic and tectonic settings within the contiguous US:

- Northern Appalachians: Large areas of crystalline rocks are exposed across much of upstate New York, New Hampshire, and Vermont. The Adirondacks crystalline rocks are part of a shield area.
- Central and Southern Appalachians: Tectonically exposed Precambrian rocks forming considerable topography in the southeastern states of Virginia through Georgia. They are generally deformed and metamorphosed.
- Central Midwest: Tectonically exposed crystalline basement rocks that form the Ouachita Mountains magmatic province of southern Oklahoma and the Llano uplift of central Texas.
- Northern Midwest: Large areas of Wisconsin and Minnesota that contain Precambrian crystalline rocks that are part of the southern Canadian Shield.
- Rocky Mountains: Mountain ranges running from the Canadian border to central New Mexico containing extensive Proterozoic crystalline-rock terrains.
- Basin and Range: Region containing Proterozoic and Phanerozoic crystalline-rock terrains that are highly faulted and covered by Tertiary volcanic rocks.
- Pacific Coast and the Sierra Nevada: A large region of the western US with outcrops of crystalline rock from the Mexican border through California and the length of the Sierra Nevada. Blocks also occur along the coast south of San Francisco and across the California-Oregon border. The Cordilleran batholiths are marginal to Precambrian basement.

Surface exposures for granitic rock in the contiguous United States based on data from Garrity and Soller (2009), a digital database of the geology of North America, are shown in Figure 4-1 (see also Perry et al. 2014) The surface exposures are color coded by surface slope. In addition, extent of previous glaciation is marked. Glaciation is a potential disruptive event for granitic repositories (see Section 5.3).

The groundwater flow pattern is a key characteristic to specify when developing a reference case. In general, the groundwater table and flow patterns are controlled by geology, recharge, and surface topography. In regions where the groundwater recharge is relatively large, bedrock permeability is relatively small, and surficial deposits overlying the bedrock are relatively thin, the groundwater table is largely controlled by surface topography. That situation is the case for regions of Sweden and Finland that have been evaluated as potential sites for crystalline repositories. Gleeson et al. (2013) have delineated regions in the US where the groundwater table is likely to be controlled by topography (Figure 4-2). Note that there is significant overlap between the location of crystalline rock (Figure 4-1) and the topography-controlled regions.

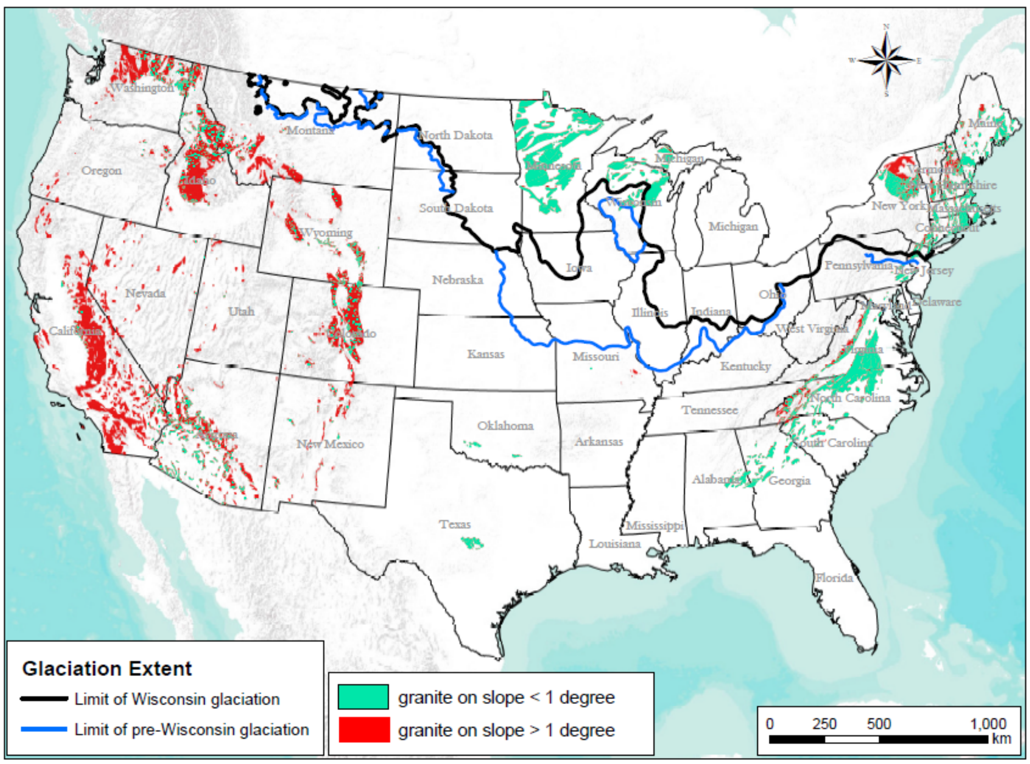

Figure 4-1. Location of crystalline rock surface exposures in the conterminous US.

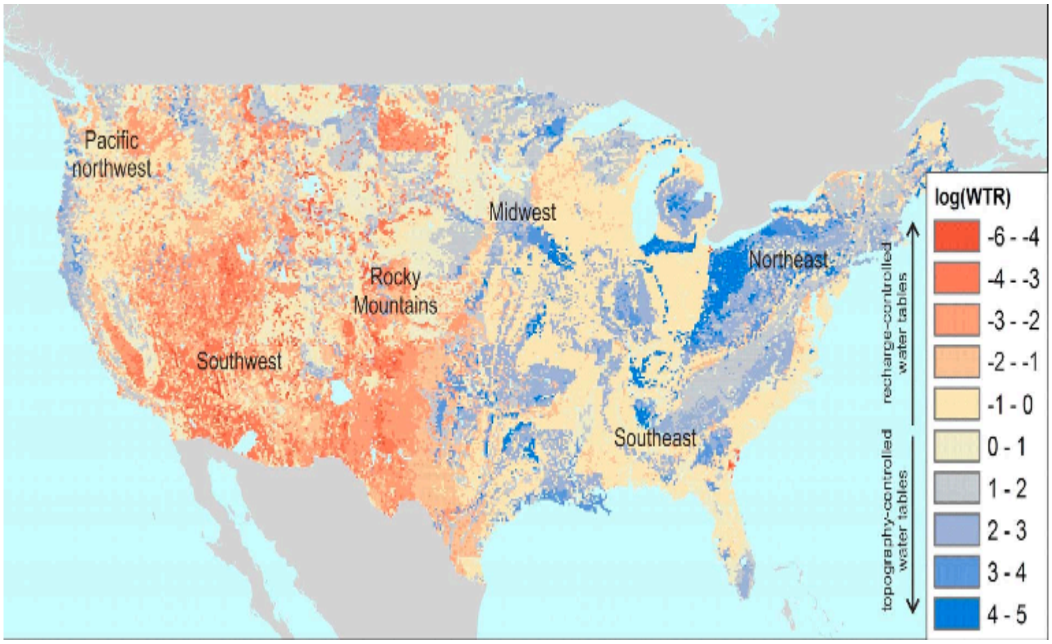

Figure 4-2. Regions where the groundwater system is likely to be controlled by topography. Figure modified from Gleeson et al. (2011). The WTR ratio is a dimensionless parameter that quantifies the relative importance of topography and recharge in controlling the water table. In areas with positive values of log(WTR), groundwater flow is topography controlled and regional contributions to flow are likely to be insignificant.

Based on the overlap between the areas with topography-controlled groundwater flow systems in Figure 4-2 and the location of surface exposures for crystalline rock (Figure 4-1), the natural system for the granite reference case is chosen to have a topography-controlled flow system, which is regarded as local flow within by Tóth's classical schema (Tóth, 1963) for topography-driven flow. The geometry for the generic natural system is shown in Figure 4-3. The site has a constant infiltration of 100 mm/y along the top and side of a hill and discharge to a topographically depressed region representing a shallow lake. The infiltration forces flow through the hypothetical repository location. Flow to the depression is enhanced by the presence of an intensely fractured deformation zone with enhanced porosity and permeability. Such zones are common in crystalline rock and represent an important feature to be considered. Typical streamlines from the repository to discharge locations in a flow configuration similar to that of Figure 4-3 are shown in Figure 4-4 (Harp, et al. 2012). These streamlines were developed from a numerical model that treated the permeability as a random space function (Harp et al. 2012).

In addition to the material zones shown in Figure 4-3, it is recommended to include surficial deposits of 1-2 m thickness at the discharge location. Although not necessarily significant in terms of groundwater travel times, radionuclides may sorb on such sediments increasing the radionuclide transport times.

Bulk permeability for fractured crystalline rock are typically in the 10^{-18} m^2 to 10^{-11} m^2 range (Bruce, 1980) but can be 10^{-12} m^2 or higher at spatial scales relevant for model grid cells (Clauser, 1992). For modeling the well-characterized Forsmark site, bulk permeability values in the range 3×10^{-16} m^2 to 10^{-14} m^2 were recommended (SKB, 2010a) for rock types other than those on the primary transport pathways, which were modeled by discrete fracture network approach. SKB (2010a) also recommended a value of 10^{-5} for fracture kinematic porosity and flow wetted specific surface area of ~0.5 m^2/m^3. Bulk flow properties recommended for generic modeling using a continuum porous medium approach are shown in Table 4-1. Parameters in a preliminary discrete fracture network model for DFN modeling of a generic site are shown in Figure 4-2. It is important to note that these parameters are highly site-specific; thus, sensitivity studies about these generic values are recommended.

Table 4-1. Bulk properties for use in generic continuum porous medium flow and transport models

Permeability Range	Kinematic Porosity	Specific Flow Wetted Surface Area
10^{-16} m^2 to 10^{-14} m^2	10^{-5}	0.5 m^2/m^3

Table 4-2. Parameters for generic modeling using discrete fracture network approaches.

Set	Orientation Distribution: Fisher			Size Distribution: Truncated Power Law			Fracture Density
	Mean Trend	Mean Plunge	Concentration κ	Exponent α	Upper cutoff R_x, m	Lower cutoff R_0, m	Number of fractures in 1 km^3
1. (NS)	90.0°	0.0°	22	2.5	500	15	2100
2. (NE)	135.0°	0.0°	22	2.7	500	15	2000
3. (HZ)	360.0°	90.0°	10	2.4	500	15	2300

Important processes to be considered in the natural system barrier include groundwater flow in fractures and deformation zones, advective transport and longitudinal dispersion of radionuclides within fractures, mixing at fracture intersections, and radionuclide retention by diffusion into rock matrix with sorption on matrix mineral grains. Values for matrix properties and groundwater chemistries compiled from various sources are provided in Appendix A.

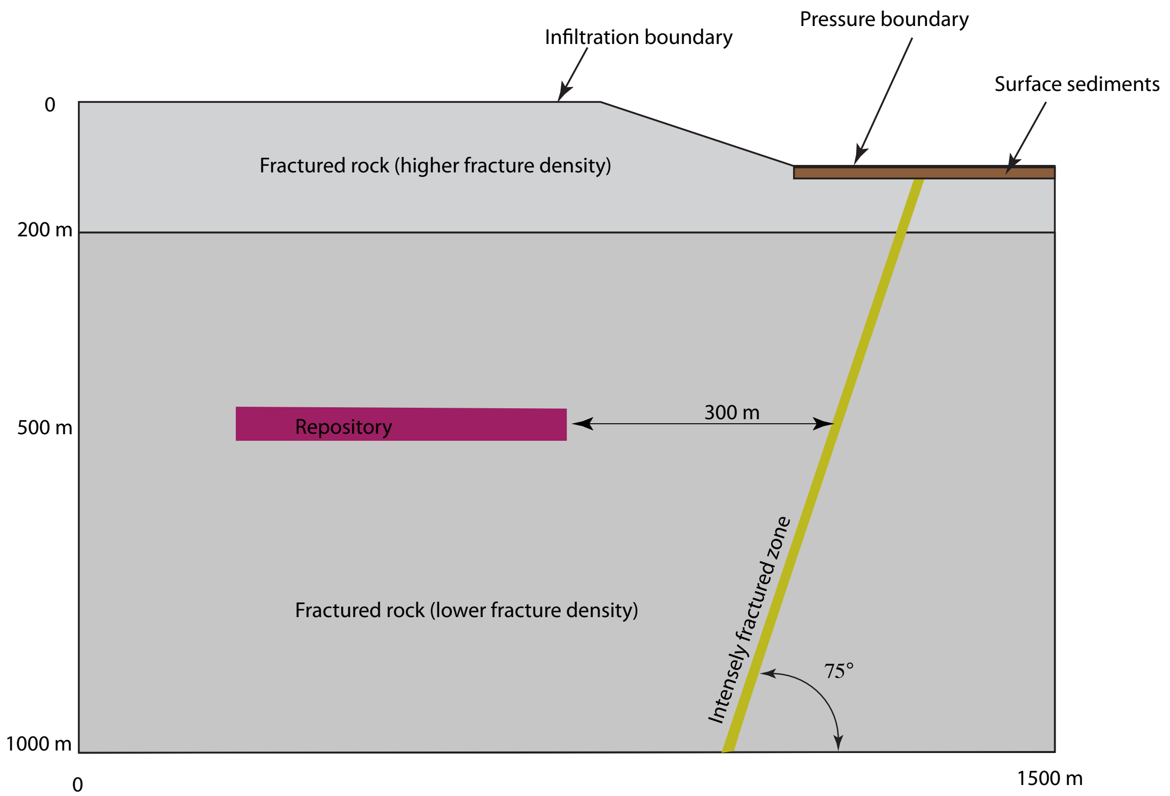

Figure 4-3. Flow configuration for generic natural system (not to scale).

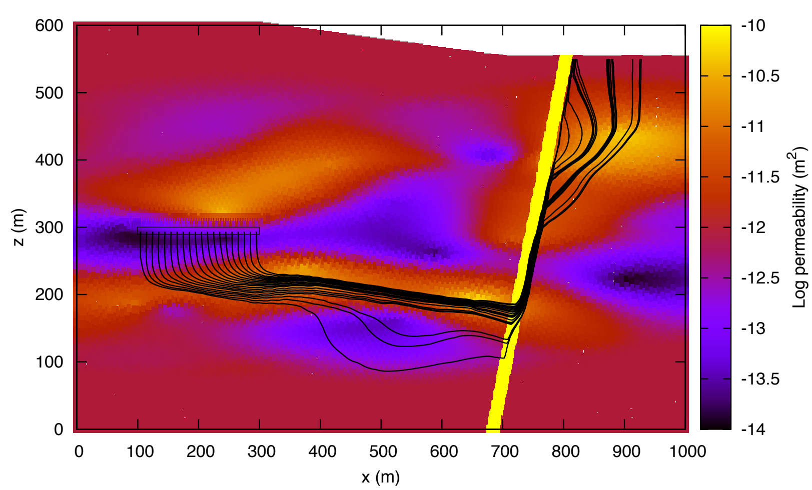

Figure 4-4. Simulated flow paths from the repository to the ground surface (Harp et al. 2013) in a configuration similar to that of Figure 4-3.

5. REFERENCE SCENARIOS

As opposed to other media, disposal in crystalline rock relies more heavily on the EBS to contain radionuclides. A principal function of the geosphere is to provide benign conditions for the EBS. A critical step in evaluating generic disposal systems is the specification of potential failure modes for the EBS. The detailed specification of failure modes is highly dependent on the local site conditions and repository design. For example, the KBS-3 concept depends on a nearly oxygen free copper canister that has low-to-negligible corrosion rates in reducing conditions. For that emplacement concept, disruptive events or manufacturing error are mechanisms that could lead to radionuclide release into the geosphere. For the emplacement-in-tunnel concept, however, the stainless steel package and carbon steel overpack are expected to degrade. Thus, we define three scenarios, depending on the emplacement concept and whether the repository is sited in locations that will be susceptible to disruptive events triggered by future glaciation (see Figure 4-1). In all three scenarios, transport in the geosphere is governed by similar processes, with the only difference being the potential for transient flow and chemistry in the glacial scenario.

5.1 Nominal Scenario (Tunnel Emplacement Concept)

Generalized or localized corrosion of the stainless steel package and carbon steel overpack are potentially important processes to consider for the emplacement-in-tunnel concept. In evaluating the rate and timing of such corrosion, the effect of the waste form and concrete lining on the chemical conditions and corrosion potential and rate should be considered. In the nominal scenario, buffer function remains intact. In addition, the resulting corrosion products may provide additional retention capacity through sorption.

5.2 Manufacturing Defect (KBS-3 Concept)

The KBS-3 concept depends on corrosion resistant copper canisters to contain waste for very long periods. An informative scenario to evaluate in this case is the situation where one or more waste packages has an initial defect. SKB’s stylized treatment of that scenario presumes transport through a small-diameter penetration (pinhole) for a period of 1000 years following the time of repository closure. At 1000 years post-closure, the penetration is assumed to rapidly expand and lead to loss of the waste package containment function. The buffer remains intact and provides a diffusion/sorption barrier for radionuclides.

5.3 Buffer Erosion Driven by Glaciation Events (Both Concepts)

The buffer erosion disruptive event is relevant for crystalline repositories sited in regions that will be subject to future glaciation events (see Figure 4-1). In this scenario, the passage of an ice sheet over the repository creates transient high infiltration, which may cause large flows of low ionic-strength water at repository depths. The low ionic-strength water then attacks the buffer eventually leading to erosion and localized loss of buffer barrier function.

6. MODELING APPROACHES

Assessments of EBS degradation and transport processes when evaluating repositories in crystalline rock require similar approaches to that of argillite/shale, with the most significant difference being that groundwater flow rates at repository depths are expected to be highly heterogeneous in crystalline rock, which should be taken into account. To account for this spatial heterogeneity in flow and resulting effects on radionuclide transport, specialized modeling approaches are required.

Fractures are ubiquitous in crystalline rock and provide the primary migration pathways for radionuclides. Experience has shown that flow and transport in fractured rock are rarely represented adequately by uniform or mildy nonuniform isotropic continuum representations (Neuman 2005) and a range of alternatives to the classical continuum representation have been developed. These alternative approaches may be grouped into three general classes: discrete fracture network representations, complex continua representations, and hybrid representations.

Discrete fracture network (DFN) models depict the rock mass as an interconnected network of explicitly represented fractures. The approach is in the reductionist tradition, implicitly assuming that detailed statistical descriptions of small observable features will, once combined in numerical simulations, lead to understanding of the system as a whole. Networks of fractures are first stochastically generated using a stochastic model derived from site data. A computational mesh is placed on each fracture plane usually ensuring that the mesh on each of a pair of intersecting fractures matches along the intersection. Groundwater flow equations are then solved using this computational mesh. The final step is then to simulate radionuclide transport using the computed flow field, usually by particle tracking. Most large-scale applications do not explicitly mesh the matrix volumes between adjacent fractures. Instead the effects of diffusion into the unrepresented matrix volume are represented (modeled) in the transport step (see e.g. Painter et al. 2008). DFN simulations were introduced first in theoretical studies; feasibility of detailed site-specific applications has also been clearly demonstrated (e.g. Cvetkovic et al. 2004, SKB 2011).

Complex continua representations generalize a simple effective continuum representation to account for various flow and transport phenomena. Dual continuum models (Barenblatt et al. 1960; Warren and Root 1963) represent fractured porous rock as two overlapping and interacting continua. In its most general form (e.g. Duguid and Lee, 1977), known as the dual permeability model, flow and transport takes place in both the fracture and matrix continua while accounting for fluid and solute migration between the two continua in response to pressure and concentration differences. Commonly, flow in the matrix system is neglected relative to flow in the fracture system. In this case, the matrix acts as a non-conductive reservoir for fluid and/or solute storage and the fracture system provides the fluid migration pathways. In this variant, usually referred to as the dual porosity model, fluid and solute flux are proportional to the pressure and concentration differences between the two continua at a given location and time. The dual continuum class of models has also been generalized (Pruess and Narasimhan 1985; Zyvoloski et al. 2008) to better represent gradients internal to the matrix blocks. In this approach, multiple continua are used to represent matrix processes. Flow between spatially adjacent matrix cells may be included or not represented, depending on the variant.

Regardless of how the matrix/fracture interactions are represented, multiple continuum models originally conceptualized the fracture flow system as having a representative elementary volume (REV) that establishes a spatial scale above which the flow properties become approximately independent of scale. For natural fracture patterns, which often have a broad distribution of fracture lengths, the existence of a classical REV scale may be questionable. Neuman proposed a stochastic continuum approach that does not require an REV (Neuman 1987, 2005). In his approach, an effective permeability tensor and other required flow/transport properties are assigned to each grid block in a conventional continuum conceptualization. However, the properties vary from grid cell to grid cell according to a stochastic model. Moreover, the stochastic model is dependent on the size of the grid block. Thus, a different stochastic model is required if the spatial discretization is changed. Parameterization of a stochastic continuum model, which generally requires inverse modeling of multiple pressure interference and solute tracer tests, has been demonstrated at the Apache Leap field site (e.g. Neuman 2005). The stochastic continuum model may be combined with any of the dual or multiple continua ideas to represent fracture/matrix interactions.

Hybrid methods adopt a reductionist view similar to DFN models but also use continuum representations for practical computational reasons (e.g. to reduce the overall size of the computational mesh). Hybrid methods fall into two subclasses: nested and upscaled. In nested models, explicit DFN models are used along transport pathways or in other regions where high spatial resolution is required and continuum representations are used in regions that are of less interest. This approach allows for a DFN representation of transport in and near expected transport pathways while still modeling a sufficiently large region to honor natural hydraulic boundary conditions. In upscaled models, explicit DFN representations are constructed and stochastically generated. However, the flow problem is not solved on the full DFN. Instead, the DFN is used to establish, grid block by grid block, equivalent permeability tensors for use in a continuum model. Jackson et al. (2000), Svensson (2001) and Botros et al. (2008) provide examples of upscaling algorithms for the permeability tensors. Experience with upscaled models for flow has generally been good, but the approach is questionable for transport. Extensions that attempt to recover the transport effects of subgrid velocity variability through stochastic simulation have emerged (Painter and Cvetkovic 2005) but have not been fully explored.

Experience suggests that it should be possible to model a sufficiently well-characterized site in a variety of ways and that combinations of methods may allow for the most efficient use of available information. Extensive studies by the Swedish Nuclear Fuel and Waste Management Company in support a safety case for a proposed spent fuel repository (SKB 2011) has clearly demonstrated practical utility of hybrid approaches to flow and transport modeling. Given this experience, DFN and DFN/continuum hybrids are expected to play an important role in future assessments of fractured hard rock sites.

For situations where the groundwater flow is adequately approximated as steady, a multistep procedure has been established (e.g. SKB 2010b).

1. Model groundwater flow using a "fracture-aware" approach. This might involve only a DFN representation of the fractured rock, but in most applications a hybrid approach will likely be needed to allow the modeling domain to be large enough to intersect natural boundaries for regional groundwater flow. A hybrid approach may use permeability tensors upscaled from DFN models in an equivalent continuum porous medium (ECPM) representation or an explicit DFN representation embedded in an ECPM. In either case, experience has shown (e.g. Selroos and Painter, 2012) that the effect of repository tunnels and intensely fractured zones can be important and should be represented.

2. Calculation of transport pathways by streamline tracing. Hypothetical tracers that follow the groundwater flow without dispersion, diffusion, or sorption processes can be used to establish transport pathways from repository locations to potential discharge locations in the biosphere. If a DFN model is used to represent the flow, then the pathways may be established directly in the DFN-derived flow field assuming mixing at fracture intersections (Makedonska et al. 2014). If an ECPM is used to represent flow, then downscaling approaches (Painter and Cvetkovic, 2005) may be used to recover the velocity variability along the pathways, which is lost in the upscaled flow field.

3. EBS failure. Reactive transport modeling can be used to establish chemical conditions in the EBS, the rate of EBS degradation, and the times at which EBS containment function is lost. This part of the calculation is conceptually similar to that of the generic argillite/shale repository and is not discussed further here.

4. EBS transport after failure. A partially failed EBS may still provide significant radionuclide retention function through sorption, diffusion, and mineral precipitation. Three-dimensional radionuclide transport calculations should include those processes, which are similar to the argillite/shale repository situation. One potential complication is that it is computationally difficult to explicitly resolve transport around a small-diameter penetration (manufacturing defect scenario) and that specialized subgrid modeling approaches (Cliffe and Kelly, 2006) are available to avoid the very fine grid resolution that would be required.

5. Radionuclide transport on the pathways. Radionuclide transport on the geosphere transport pathways established in Step 2 using the radionuclide releases from Step 5 is the final step. The

relevant processes are advection, longitudinal dispersion, matrix diffusion, and sorption. Radionuclide transport may be simulated in a variety of ways, including conventional finite-difference, inverse Laplace methods, or time-domain particle tracking (Painter et al. 2008). The latter method is specifically designed for this application and is computationally advantageous.

6. Biosphere. The biosphere representation depends on applicable regulations and site-specific scenarios regarding potential pathways from the geosphere to receptors of radionuclides. For the reference cases in UFDC, the biosphere conceptualization is based on the International Atomic Energy Agency (IAEA) BIOMASS Example Reference Biosphere 1B dose model (IAEA 2003), which assumes that the receptor is an individual adult who obtains drinking water from a well drilled into the aquifer above the discharge locations from the repository host rock. Dissolved radionuclide concentrations in the aquifer are converted to estimates of annual dose to the receptor (dose from each radionuclide and total dose) based on the well pumping rate, the water consumption rate of the receptor, and radionuclide-specific dose conversion factors.

7. SUMMARY

Establishment of a generic reference case specifying the emplacement concept, waste inventory, waste form, waste package, backfill/buffer properties, EBS failure scenarios, host rock properties, and biosphere is an important step in developing a baseline for model development. A generic salt repository reference case was developed in Freeze et al. (2013) and a generic argillite/shale repository reference case was presented by Zheng et al. (2014). The current report addresses the same for a generic crystalline repository, focusing on those elements of the reference case that differ from the generic salt and crystalline cases.

Three emplacement concepts were specified: a waste packages containing 4 PWR assemblies emplaced in boreholes in the floors of tunnels (KBS-3 concept), a 12-assembly waste package emplaced in tunnels, and a 32-assembly dual purpose canister emplaced in tunnels. Alternative concepts such as a borehole array drilled between upper and lower mined cavities were not considered here, but exploration of such alternative concepts would be a potential direction for future research.

Three failure scenarios were suggested for future use: a nominal scenario involving corrosion of the waste package in the tunnel emplacement concepts, a manufacturing defect scenario applicable to the KBS-3 concept, and a disruptive glaciation scenario applicable to both emplacement concepts.

A flow configuration for a generic natural barrier in a crystalline rock was developed, assuming that groundwater flow is controlled by topography. In the situation of topography-controlled flow, the regional contribution to flow is less important than local flow.

The computational approaches required to analyze EBS failure and transport processes in a crystalline rock repository are similar to those of argillite/shale, with the most significant difference being that the EBS in a crystalline rock repository will likely experience highly heterogeneous flow rates, which should be represented in the model. The computational approaches required to analyze radionuclide transport in the natural system are very different because of the highly channelized nature of fracture flow. Computational workflows tailored to crystalline rock based on discrete transport pathways extracted from discrete fracture network models are recommended.

8. REFERENCES

Barenblatt, G.I., Zheltov Y.P., Kochina I.N., 1960. Basic concepts in the theory of seepage of homogeneous liquids in fissured rocks. Journal of Applied Mathematics of Mechanics (English Translation) 24, 1286–1303.

Botros F. E., Hassan A. E., Reeves D. M., and Pohll G., 2008. On mapping fracture networks onto continuum, Water Resources Research 44, W08435, doi:10.1029/2007WR006092.

Bruce, W.F., 1980. Permeability of crystalline and argillaceous rocks. Int. J. Rock Mech. Min. Sci. and Geomech. Abstr. 17, 241–1251.

Clauser, C., 1992. Permeability of crystalline rocks. EOS Trans. Am. Geophys. Union 73: 233-38.

Cliffe, K. A., Kelly M., 2006. COMP23 v1.2.2 Users manual. SKB R-04-64, Svensk Kärnbränslehantering AB.

Cvetkovic V., Painter S., Outters N., and Selroos J.-O., 2004. Stochastic simulation of radionuclide migration in discretely fractured rock near Aspo hard rock laboratory, Water Resources Research 40, W02404, doi:10.1029/2003WR002655.

Duguid J.O. and Lee P. C. Y., 1977. Flow in fractured porous rock, Water Resources Research 13, 558–566.

Freeze, G., W.P. Gardner, P. Vaughn, S.D. Sevougian, P. Mariner, V. Mousseau, G. Hammond. 2013. Enhancements to Generic Disposal System Modeling Capabilities. FCRD-UFD-2014-000062; SAND2013-10532P

Garrity and Soller, 2009. Database of the Geologic Map of North America; adapted from the map by J.C. Reed, Jr. and others (2005). U.S. Geological Survey Data Series 424.

Gleeson, T., Marklund, L, Smith, L. and Manning, A. H., 2011. Classifying the water table at regional to continental scales, Geophys. Res. Lett., 38, L05401, doi:10.1029/2010GL046427.

Jackson, C., Hoch, A., Todman, S., 2000. Self-consistency of a heterogeneous continuum porous medium representation of a fractured medium, Water Resour. Res. 36 (1), 189-202.

Jové Colón, C. J. A. Greathouse, S. Teich-McGoldrick, et al., 2013. EBS Model Development and Evaluation Report, FCRD-UFD-2013-000312.

Harp, D., Chu, S., Miller, T.A. and Painter , S., 2013. *Generic Disposal System Modeling Using Amanzi: Generic Granite Repository Example.* LA-UR-13-26043. Los Alamos National Laboratory, Los Alamos, NM.

Hardin, E., Clayton, D., Howard, R., Scaglione, J.M., Pierce, E., Banerjee, K., Voegele, M.D., Greenberg, H., Wen, J., Buscheck, T.A., Carter, J.T., Severynse, T., Nutt, W.M., 2013. Preliminary Report on Dual-Purpose Canister Disposal Alternatives (FY13), August, 2013, FCRD-UFD-2013-000171 Rev. 0

IAEA (International Atomic Energy Agency) 2003. Reference Biospheres for Solid Radioactive Waste Disposal. IAEA-BIOMASS-6. International Atomic Energy Agency, Vienna, Austria.

Neuman, S. P., 1987. Stochastic continuum representation of fractured rock permeability as an alternative to the REV and discrete fracture concepts. In Farmer I.W., Daemen J. J. K., Desai C.S., Glass C.E. Neuman S. P. (eds) Rock Mechanics, Proceedings of the 28th US Symposium, Tucson, Arizona. AA Balkema, Rotterdam.

Neuman, S. P., 2005. Trends, prospects and challenges in quantifying flow and transport through fractured rocks, Hydrogeology Journal 13, 124–147.

Makedonska, M., Painter, S.L., Hsieh, T.-L., Bui, Q.M. and Gable, C.W., 2014. Particle tracking on discrete fracture network models with finite-volume meshes, in prep.

Mariner, P. E., J. Lee, E. L. Hardin, F. D. Hansen, G. A. Freeze, A. S. Lord, B. Goldstein, and R. H. Price, 2011. *Granite Disposal of U.S. High-Level Radioactive Waste.* SAND2011-6203, Sandia National Laboratories, Albuquerque, NM.

Painter S. and Cvetkovic V., 2005. Upscaling discrete fracture network simulations: An alternative to continuum transport models, Water Resources Research 41, W02002, doi:10.1029/2004WR003682.

Painter S., Cvetkovic V., Mancillas J., and Pensado O., 2008. Time domain particle tracking methods for simulating transport with retention and first-order transformation, Water Resources Research 44, W01406, doi:10.1029/2007WR005944.

Painter S., Gable C., and Kelkar S., 2011. Pathline tracing on fully unstructured control volume grids. Computational Geosciences 16(4) 1125–1134.

Perry, F. V., Kelley, R. E., Birdsell, S. M., Dobson, P. F., Houseworth, J. E., 2014. Regional Geology: A GIS Database for Alternative Host Rocks and Potential Siting Guidelines, LA-UR-14-20368. Los Alamos National Laboratory, Los Alamos, NM.

Pruess K. and Narasimhan, T.N., 1985. A practical method to modeling fluid and heat flow in fractured porous media. Society Petroleum Engineers Journal 25(1), 14–26.

SKB. 2011. Long-term safety for the final repository for spent nuclear fuel at Forsmark: Main report of the SR-Site project. SKB-TR-11-01 (3 volumes).

Selroos, J.O. and Painter, S.L. 2012. Effect of transport-pathway simplifications on projected releases of radionuclides from a nuclear waste repository (Sweden). Hydrogeology Journal 20(8), 1467–1481.

Tóth, J., 1963. A theoretical analysis of groundwater flow in small drainage basins, J. Geophys. Res., 68, 4795-4812.

SKB, 2010a. Data report for the safety assessment SR-Site. SKB TR-10-52, Svensk Kärnbränslehantering AB

SKB, 2010b. Radionuclide transport report for the safety assessment SR-Site. SKB TR-10-50, Svensk Kärnbränslehantering AB

SKB, 2011. Long-term safety for the final repository for spent nuclear fuel at Forsmark, SKB TR-11-01, Svensk Kärnbränslehantering AB

Svensson U., 2001. A continuum representation of fracture networks: Part I. Method and basic test cases, Journal of Hydrology 250, 170–186.

Zheng, L., Jove Colon, C., Bianchi, M., Birkholzer, J., 2014. Generic Argillite/Shale Disposal Reference Case. FCRD-UFDC-2014-000319

Zyvoloski G. A, Robinson B. A, Viswanathan H. S., 2008. Generalized dual porosity: A numerical method for representing spatially variable sub-grid scale processes, Advances in Water Resources 31 (3) 535–544, DOI: 10.1016/j.advwatres.2007.11.006

Appendix A: Geosphere flow and transport properties

Key granite far field parameters compiled from different sources are listed in the following tables.

Table A- 1. Sorption Coefficient – SKB1

Element	Chemical form/redox state	Non-saline Kd (m^3/kg)	Uncertainty interval	Saline Kd (m^3/kg)	Uncertainty interval
C	HCO_3 -	0.001	(0.0005-0.002)	0.001	(0.0005-0.002)
Cl	Cl -	0	-	0	-
Co	Co(II)	0.1	(0.05-0.5)	0.02	(0.01-0.1)
Ni	Ni(II)	0.1	(0.05-0.5)	0.02	(0.01-0.1)
Se	Se(-II, IV,VI)	0.001	(0.0005-0.005)	0.001	(0.0005-0.005)
Kr	inert gas	0	-	0	-
Sr	Sr(II)	0.01	(0.005-0.05)	0.0002	(0.0001-0.001)
Zr	Zr(IV)	1	(0.5-3)	1	(0.5-3)
Nb	Nb(V)	1	(0.5-3)	1	(0.5-3)
Tc	Tc(IV)	1	(0.3-3)	1	(0.3-3)
Tc	Tc(VII)	0		0	
Pd	Pd(II)	0.1	(0.01-0.5)	0.01	(0.001-0.05)
Ag	Ag(I)	0.5	(0.1-1)	0.05	(0.01-0.1)
Cd	Cd(II)	0.1	(0.05-0.5)	0.02	(0.01-0.1)
Sn	Sn(IV)	0.001	(0-0.01)	0.001	(0-0.01)
I	I-	0	-	0	-
Cs	Cs(I)	0.5	(0.1-1)	0.05	(0.01-0.1)
Sm	Sm(III)	2	(1-5)	2	(1-5)
Eu	Eu(III)	2	(1-5)	2	(1-5)
Ho	Ho(III)	2	(1-5)	2	(1-5)
Ra	Ra(II)	0.1	(0.05-0.5)	0.02	(0.01-0.1)
Ac	Ac(III)	3	(1-5)	3	(1-5)
Th	Th(IV)	5	(1-10)	5	(1-10)
Pa	Pa(IV,V)	1	(0.5-5)	1	(0.5-5)
U	U(IV)	5	(1-10)	5	(1-10)
U	U(VI)	0.01	(0.005-0.02)	0.005	(0.001-0.01)
Np	Np(IV)	5	(1-10)	5	(1-10)
Np	Np(V)	0.01	(0.005-0.05)	0.005	(0.001-0.01)
Pu	Pu(III,IV)	5	(1-10)	5	(1-10)
Am	Am(III)	3	(1-5)	3	(1-5)
Cm	Cm(III)	3	(1-5)	3	(1-5)

Data sources: Carbol and Engkvist (1997, SKB technical report R-97-13, table 12-1)

The non-saline and the saline groundwaters are represented by the type of water found at the Gideå and Äspö study site, respectively. The restrictions for the non-saline water are: pH≥7, [Cl-] < 500 mg/l and Eh< -200 mV. The restrictions for the saline water are: pH≥7, 500 mg/l < [Cl-] < 6500 mg/l and Eh< -200 mV.

Table A- 2 Sorption Coefficient – SKB2

Radionuclide (Redox State)	Best estimate Kd (m3/kg)	$\log_{10}K_d$ – μ	$\log_{10}K_d$ – σ	Lower K_d limit (m3/kg)	Upper K_d limit (m3/kg)
Ac(III)	1.48·10–2	–1.83	0.72	5.74·10–4	3.83·10–1
Ag(I)	3.49·10–4	–3.46	0.51	3.46·10–5	3.52·10–3
Am(III)	1.48·10–2	–1.83	0.72	5.74·10–4	3.83·10–1
C, HCO3 –	0	–	–	0	0
C, CH4	0	–	–	0	0
C, -CO2H	0	–	–	0	0
Cd(II)	1.10·10–3	–2.96	0.65	5.97·10–5	2.04·10–2
Cl(-I)	0	–	–	0	0
Cm(III)	1.48·10–2	–1.83	0.72	5.74·10–4	3.83·10–1
Cs(I)	3.49·10–4	–3.46	0.51	3.46·10–5	3.52·10–3
Eu(III)	1.48·10–2	–1.83	0.72	5.74·10–4	3.83·10–1
H(I)	0	–	–	0	0
Ho(III)	1.48·10–2	–1.83	0.72	5.74·10–4	3.83·10–1
I(-I)	0	–	–	0	0
Mo(VI)	0	–	–	0	0
Nb(V)	1.98·10–2	–1.70	0.64	1.11·10–3	3.53·10–1
Ni(II)	1.10·10–3	–2.96	0.65	5.97·10–5	2.04·10–2
Np(IV)	**5.29·10–2**	**–1.28**	**0.65**	**2.84·10–3**	**9.84·10–1**
Np(V)	4.13·10–4	–3.38	0.74	1.48·10–5	1.15·10–2
Pa(IV)	5.92·10–2	–1.23	0.48	6.76·10–3	5.18·10–1
Pa(V)	**5.92·10–2**	**–1.23**	**0.48**	**6.76·10–3**	**5.18·10–1**
Pb(II)	2.52·10–2	–1.60	0.56	2.05·10–3	3.10·10–1
Pd(II)	5.20·10–2	–1.28	0.83	1.22·10–3	2.21
Pu(III)	**1.48·10–2**	**–1.83**	**0.72**	**5.74·10–4**	**3.83·10–1**
Pu(IV)	5.29·10–2	–1.28	0.65	2.84·10–3	9.84·10–1
Pu(V)	9.14·10–3	–2.04	0.6	6.19·10–4	1.35·10–1
Pu(VI)	9.14·10–3	–2.04	0.6	6.19·10–4	1.35·10–1
Ra(II)	2.42·10–4	–3.62	0.41	3.87·10–5	1.51·10–3
S(-II)	0	–	–	0	0
Se(-II)	**2.95·10–4**	**–3.53**	**0.55**	**2.50·10–5**	**3.48·10–3**
Se(IV)	2.95·10–4	–3.53	0.55	2.50·10–5	3.48·10–3
Se(VI)	2.95·10–4	–3.53	0.55	2.50·10–5	3.48·10–3
Sm(III)	1.48·10–2	–1.83	0.72	5.74·10–4	3.83·10–1
Sn(IV)	1.59·10–1	–0.80	0.28	4.51·10–2	5.58·10–1
Sr(II)	3.42·10–6	–5.47	0.99	3.84·10–8	3.05·10–4
Tc(IV)	**5.29·10–2**	**–1.28**	**0.65**	**2.84·10–3**	**9.84·10–1**
Tc(VII)	0	–	–	0	0
Th(IV)	5.29·10–2	–1.28	0.65	2.84·10–3	9.84·10–1
U(IV)	**5.29·10–2**	**–1.28**	**0.65**	**2.84·10–3**	**9.84·10–1**
U(VI)	**1.06·10–4**	**–3.97**	**0.66**	**5.53·10–6**	**2.05·10–3**
Zr(IV)	2.13·10–2	–1.67	0.35	4.48·10–3	1.02·10–1

Data sources: SKB technical report TR-10-50, Table 2-4. K_d values for use in SR-Site simulations of the Forsmark site. The predominant species for redox sensitive elements are highlighted in bold text. Values are given for the best estimate (median), parameters for the lognormal distribution (μ and σ), as well as lower and upper limits corresponding to the 2.5% and 97.5% percentiles, respectively.

Table A- 3 Sorption Coefficient – JAEA

Species	Data (range) (unit: cc/g)	Geometric mean (cc/g)	Geometric STDV (dimensionless)	Mean of log10(data) data unit (m^3/kg)	STDV of log10(data)
Am	220 - 190000	9096.03	4.306	0.959	0.634
Pu	0.2 - 401000	1736.9	13.957	0.24	1.145
Np	0.65 - 2720	31.61	5.667	-1.5	0.753
U	0 - 280000	16.04	9.215	-1.795	0.965
Tc	0.1 - 200000	15.5	56.54	-1.81	1.752
Sn	173 - 2940	688.4	2.754	-0.162	0.44
Cs	1 - 131000	135.76	7.991	-0.867	0.903
I	0.5 – 1.9	0.89	1.43	-3.052	0.155
Se	0 - 18	2.63	3.114	-2.579	0.493
Th	501 - 10000	1245.51	2.322	0.095	0.366
Pa	2.4 – 7.3	4.14	1.558	-2.383	0.193
Ra	30.1 - 3800	504.84	4.302	-0.297	0.634
Pb	1600 - 4400	2653.3	1.658	0.424	0.22
Sr	1 - 880	20.87	3.785	-1.68	0.578
Sb	450 - 519	483.27	1.074	-0.316	0.031
Zr	2.6 - 3160000	839.02	12.746	-0.076	1.105
Nb	7 - 142000	465.596	4.996	-0.332	0.699
Ac	83 - 40000	6687.15	8.17	0.825	0.912
Pd	142 - 82800	2256.63	5.301	0.353	0.724

Note: Data with de-ionized and other water chemistry that are obviously not relevant are not included except for Ac and Pd. For these two species no other data are available.

Data sources: Japan JAEA database: http://migrationdb.jaea.go.jp/english.html

Table A- 4. Sorption Coefficient – SNL

Element	Kd (m^3/kg
C, Cl, I	0
Se	0.0005
Pd, Sn	0.001
Sr	0.005
Nb	0.02
Am, Cm, Ac	0.04
Pa, Tc, Cs	0.05
Sb	0.1
U	0.1
Np, Th, Ra, Zr	0.2
Pu	0.5
Pb	1

Data sources: Mariner et al. (2011), table 2-3.

Table A- 5. Solubility – SNL

Element	Solubility	Units
Actinium (Ac)	6.00E-06	mol/L
Americium (Am)	6.00E-06	mol/L
Carbon (C)	1.00E+50	mol/L
Curium (Cm)	6.00E-06	mol/L
Cesium (Cs)	1.00E+50	mol/L
Iodine (I)	1.00E+50	mol/L
Niobium (Nb)	4.00E-05	mol/L
Neptunium (Np)	1.00E-09	mol/L
Protactinium (Pa)	1.00E-09	mol/L
Lead (Pb)	1.00E+50	mol/L
Paladium (Pd)	3.00E-06	mol/L
Plutonium (Pu)	2.00E-07	mol/L
Radium (Ra)	1.00E-06	mol/L
Antimony (Sb)	1.00E-07	mol/L
Selenium (Se)	4.00E-08	mol/L
Tin (Sn)	3.00E-08	mol/L
Strontium (Sr)	1.00E+50	mol/L
Technetium (Tc)	3.00E-08	mol/L
Thorium (Th)	4.00E-07	mol/L
Uranium (U)	4.00E-10	mol/L
Zirconium (Zr)	2.00E-08	mol/L

Note: no limit represented by 1E+50 mol/L
Data sources: Mariner et al. (2011), table 2-5 (pH 7.5, T = 25 deg C).
C, Cs, I, Sr, and Pb assumed infinitely soluble.

Table A- 6. Solubility – SKB

Element	Solubility	Unit
Ac-227	$1.00 \cdot 10^{17}$	mol/L
Ag-108m	$1.10 \cdot 10^{-5}$	mol/L
Am-241	$2.50 \cdot 10^{-6}$	mol/L
Am-242m	$2.50 \cdot 10^{-6}$	mol/L
Am-243	$2.50 \cdot 10^{-6}$	mol/L
C-14	$1.00 \cdot 10^{17}$	mol/L
Cd-113m	$1.00 \cdot 10^{17}$	mol/L
Cl-36	$1.00 \cdot 10^{17}$	mol/L
Cm-245	$2.60 \cdot 10^{-6}$	mol/L
Cm-246	$2.60 \cdot 10^{-6}$	mol/L
Cs-135	$1.00 \cdot 10^{17}$	mol/L
Cs-137	$1.00 \cdot 10^{17}$	mol/L
Eu-152	$1.00 \cdot 10^{17}$	mol/L
H-3	$1.00 \cdot 10^{17}$	mol/L
Ho-166m	$4.10 \cdot 10^{-6}$	mol/L
I-129	$1.00 \cdot 10^{17}$	mol/L
Mo-93	$1.00 \cdot 10^{17}$	mol/L
Nb-93m	$4.90 \cdot 10^{-5}$	mol/L
Nb-94	$4.90 \cdot 10^{-5}$	mol/L
Ni-59	$3.00 \cdot 10^{-4}$	mol/L
Ni-63	$3.00 \cdot 10^{-4}$	mol/L
Np-237	$1.00 \cdot 10^{-9}$	mol/L
Pa-231	$3.30 \cdot 10^{-7}$	mol/L
Pb-210	$1.70 \cdot 10^{-6}$	mol/L
Pd-107	$3.90 \cdot 10^{-6}$	mol/L
Pu-238	$4.80 \cdot 10^{-6}$	mol/L
Pu-239	$4.80 \cdot 10^{-6}$	mol/L
Pu-240	$4.80 \cdot 10^{-6}$	mol/L
Pu-242	$4.80 \cdot 10^{-6}$	mol/L
Ra-226	$9.10 \cdot 10^{-7}$	mol/L
Se-79	$6.70 \cdot 10^{-9}$	mol/L
Sm-151	$1.10 \cdot 10^{-7}$	mol/L
Sn-121m	$9.00 \cdot 10^{-8}$	mol/L
Sn-126	$9.00 \cdot 10^{-8}$	mol/L
Sr-90	$3.70 \cdot 10^{-3}$	mol/L
Tc-99	$3.80 \cdot 10^{-9}$	mol/L
Th-229	$2.60 \cdot 10^{-9}$	mol/L
Th-230	$2.60 \cdot 10^{-9}$	mol/L
Th-232	$2.60 \cdot 10^{-9}$	mol/L
U-233	$9.50 \cdot 10^{-10}$	mol/L
U-234	$9.50 \cdot 10^{-10}$	mol/L
U-235	$9.50 \cdot 10^{-10}$	mol/L
U-236	$9.50 \cdot 10^{-10}$	mol/L
U-238	$9.50 \cdot 10^{-10}$	mol/L
Zr-93	$1.80 \cdot 10^{-8}$	mol/L

Data sources: SKB technical report TR-10-50, Table 3-4, for temperate condition.

Note: $1.x10^{17}$ represents unlimited solubility.

Table A- 7. Diffusivity - JAEA

Species	De : effective diffusivity (range) (unit: m^2/s)	Dp : pore diffusivity (range) (unit: m^2/s)	Mean (Dp)	Standard Deviation (Dp)
Am				
Pu	$1.28e^{-13} – 2.76e^{-13}$	$2.61e^{-11} – 5.63e^{-11}$	4.10E-11	1.07E-11
Np	$2.10e^{-13} – 5.41e^{-13}$	$2.80e^{-11} – 1.10e^{-10}$	6.99E-11	2.75E-11
U	$2.20e^{-14} – 4.40e^{-14}$	$3.14e^{-12} – 6.29e^{-12}$	5.14E-12	1.42E-12
Tc	$4.20e^{-14} – 4.20e^{-14}$	$4.20e^{-12} – 4.20e^{-12}$	4.20E-12	0
Sn				
Cs	$5.04e^{-13} – 1.80e^{-11}$	$1.03e^{-10} – 3.75e^{-10}$	2.11E-10	1.05E-10
I	$3.90e^{-13} – 2.60e^{-12}$	$7.96e^{-11} – 3.38e^{-10}$	1.57E-10	6.02E-10
Se	$1.90e^{-12} – 5.30e^{-12}$	$8.26e^{-11} – 9.46e^{-11}$	8.93E-11	5.00E-12
Th				
Pa				
Ra				
Pb				
Sr	$2.00e^{-13} – 1.60e^{-12}$	$2.86e^{-11} – 4.00e^{-10}$	6.65E-11	9.66E-11
Sb				
Zr				
Nb				
Ac				
Pd				

Note: Dp (pore diffusivity) (Dp = De/porosity) is generally used in dual-porosity model as matrix diffusion coefficient. Data with de-ionized water are not included. Blank line means no data available.
Data sources: Japan JAEA database: http://migrationdb.jaea.go.jp/english.html

Table A- 8. Various Far Field Parameters

SKB technical report TR-10-52, table 6-91

Parameter Description	Value	mean	Stdv	Units	Distribution Type	Index
Bulk Density	2700			kg/m3		1
Porosity	0.0018			[]		2
permeasbility	10^{-20} to 10^{-19}			m^2		3
Longitude dispersivity	50			m		4
Equivalent flow rate	$4.2x10^{-6}$ to $1.2x10^{-4}$			m^3/yr		5
Colloid concentrations	10			mg/l		6
Colloid concentrations (with dilute glacial melt water)	10			g/l		7
Hydraulic conductivity (for depth 200 to 400 m)	$3x10^{-9}$ to $1x10^{-7}$			m/s		8
Hydraulic conductivity (for depth > 400 m)	10^{-13} to 10^{-10}			m/s		9
Fracture zone mean fracture aperture	$5x10^{-4}$			m		10
Fracture aperture	10^{-5} to $3x10^{-3}$			m		11
Fractutre spacing	0.25 to 15			m		12
Fracture length	1.5 to 76			m		13
Heat conductivity	2.77 to 3.34			$W\ m^{-1}\ K^{-1}$		14
Heat capacity	2.17 to 2.24			$MJ\ m^{-3}\ K^{-1}$		15
	Best estimate	**$Log_{10}D_e$ (m^2/s)**	**$Log_{10}D_e$ (m^2/s)**			
Effective diffusivity (cations, non-charged solutes)	$2.1x10^{-14}$	-13.7	0.25	m^2/s	Log-normal	16
Effective diffusivity (anions)	$6.6x10^{-15}$	-14.2	0.25	m^2/s	Log-normal	17

Data sources:

1. SKB technical report TR-10-52, Table 3-2
2. SKB technical report TR-10-52, Table 3-2
3. Sandia report SAND2011-6203, p75-76
4. SKB technical report TR-10-52, Table 6-85
5. SKB technical report TR-10-50, Table 3-5
6. SKB technical report TR-10-50
7. SKB technical report TR-10-50
8. SKB technical report TR-10-52, Table 6-78
9. Sandia report SAND2011-6203, Table 1-3
10. Posiva 2010. Models and Data Report 2010. POSIVA 2010-01. Posiva Oy, Olkiluoto, Finland.
11. Kalinina et al. Paper "Analysis of the Effect of Heterogeneity on Heat Extraction in an EGS Represented with the Continuum Fracture Model", data from granite sites in US, Czech Republic, France, Spain, Portugal, Sweden, Egypt and Japan.
12. Kalinina et al. Paper "Analysis of the Effect of Heterogeneity on Heat Extraction in an EGS Represented with the Continuum Fracture Model", data from granite sites in US, Czech Republic, France, Spain, Portugal, Sweden, Egypt and Japan.
13. Kalinina et al. Paper "Analysis of the Effect of Heterogeneity on Heat Extraction in an EGS Represented with the Continuum Fracture Model", data from granite sites in US, Czech Republic, France, Spain, Portugal, Sweden, Egypt and Japan.
14. based on values at Forsmark and Laxemar (SKB 2006, Table 9-4)
15. based on values at Forsmark and Laxemar (SKB 2006, Table 9-4)
16. SKB technical report TR-10-52, Table 6-91
17. SKB technical report TR-10-52, Table 6-91

Table A- 9 Global Transport Parameters

	Median	5 percentilce	95 percentile	Unit
Hydrodynamic Transport Resistance Parameter (F)	4.00E+06	3.00E+05	1.00E+08	yr/m
Travel time	150	30	1000	yr

Note: 500 m travel distance. Should be scaled to other values.

Data sources: SKB technical report TR-10-52, Figure 6-67; Painter, S., Cvetkovic, V., Mancillas, J., Pensado, O. (2008): Time domain particle tracking methods for simulating transport with retention and first-order transformation. Water Resources Research 43(9), W01406; SKB. 2010. Radionuclide transport report for the safety assessment SR-Site. SKB Technical Report TR-10-50. Swedish Nuclear Fuel and Waste Management Co.

The parameters hydrodynamic transport resistance and global travel time are integrated quantities of a flowpath/streamline. Within some models of radionuclide transport (e.g. Painter et al., 2008 and SKB, 2010), these two parameters are the only flow related parameters controlling radionuclide transport. The transport resistance parameter is the flow-rate normalized flow-wetted surface area of a streamtube of infinitesimal cross-section. It is denoted beta in Painter et al. (2010) and F in SKB (2010). The global travel time is the travel time of a non-dispersing, non-sorbing, non-diffusing tracer moving with the groundwater flow.

Table A- 10. Groundwater Composition from various sites

Parameter	Olkiluoto, Finland	Olkiluoto, Finland	Olkiluoto, Finland	Laxemar, Sweden	Forsmark, Sweden	Pinawa, Canada	East Bull Lake, Canada
Borehole	OL-KR20	OL-KR10	OL-KR12	KLX03	KFM02A	WN-4	EBL-2
Depth (m)	360	487	708	380	512	513	538
TDS (g L^{-1})	10.5	22.1	49.5	2.8	9.3	7.5	2.3
Ionic strength (eq L^{-1})	0.22	0.48	1.18	0.05	0.19	0.16	0.05
pH	7.4	8	8.2	7.9	7.2	8.1	7.4
Na (mol L^{-1})	0.11	0.21	0.36	0.03	0.09	0.07	0.03
Ca (mol L^{-1})	0.03	0.09	0.25	0.01	0.02	0.03	0.01
K (mol L^{-1})	2.8E-04	3.6E-04	4.9E-04	1.4E-04	9.0E-04	5.3E-04	5.4E-05
Mg (mol L^{-1})	2.6E-03	1.6E-03	1.5E-03	4.4E-04	9.3E-03	1.1E-03	7.0E-05
Sr (mol L^{-1})	1.6E-04	3.7E-04	1.1E-03	nr	nr	nr	3.3E-05
Mn (mol L^{-1})	5.8E-06	7.3E-06	9.3E-06	nr	nr	nr	nr
Cl (mol L^{-1})	0.18	0.38	0.86	0.04	0.15	0.11	0.04
SO4 (mol L^{-1})	2.1E-04	1.0E-05	5.0E-05	1.3E-03	5.2E-03	6.6E-03	1.4E-04
CO3 (mol L^{-1})	5.5E-04	1.1E-04	4.0E-05	3.1E-03	2.2E-03	3.5E-03	5.0E-04
SiO2 (mol L^{-1})	3.6E-04	2.8E-04	2.1E-04	nr	nr	nr	5.4E-05
Fe (mol L^{-1})	2.5E-06	2.0E-06	3.8E-07	8.0E-06	3.3E-05	nr	nr
S(-II) (mol L^{-1})	5.6E-06	<3.1 E-7	1.3E-06	3.0E-07	0.0E+00	nr	nr
Reference	Posiva (2010), Table 6-6	Posiva (2010), Table 6-6	Posiva (2010), Table 6-6	SKB (2006d), p. 382	SKB (2006d), p. 382	Gascoyne et al. (1987), Table 3	Gascoyne et al. (1987), Table 3

Note: nr =not reported
Data sources: Mariner et al. (2011), table 2-1 Sample groundwater composition in granite at depths from 360 to 708 m.

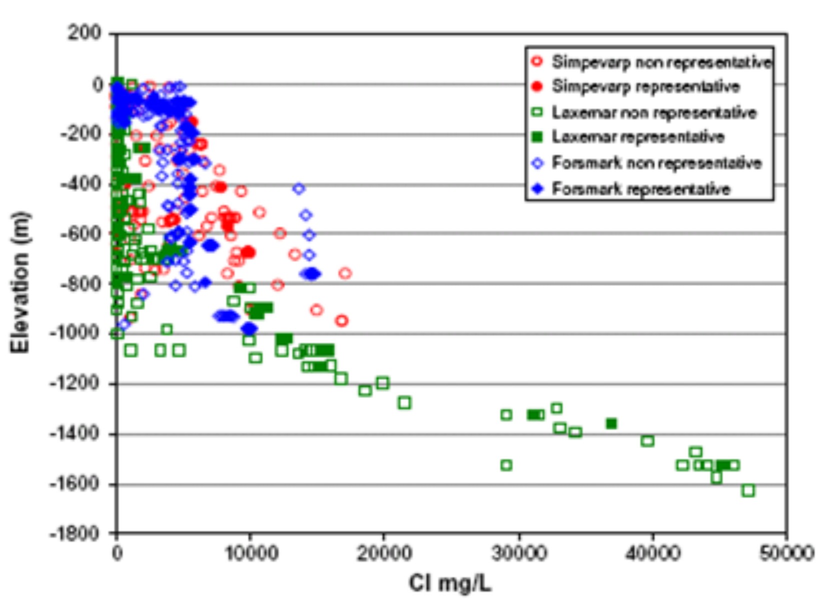

Figure A- 1. Chloride distribution with depth for Swedish granite sites (Laaksoharju et al., 2008): Laxemar (green), Simpevarp (red), Forsmark (blue). Open symbols represent samples considered unsuitable. Elevation indicated above sea level. Note: Chloride charge is balanced almost entirely by Na+ and Ca2+ (the sum of the concentrations of these two ions should be approximately 4/7ths that of Cl- in mg/L).

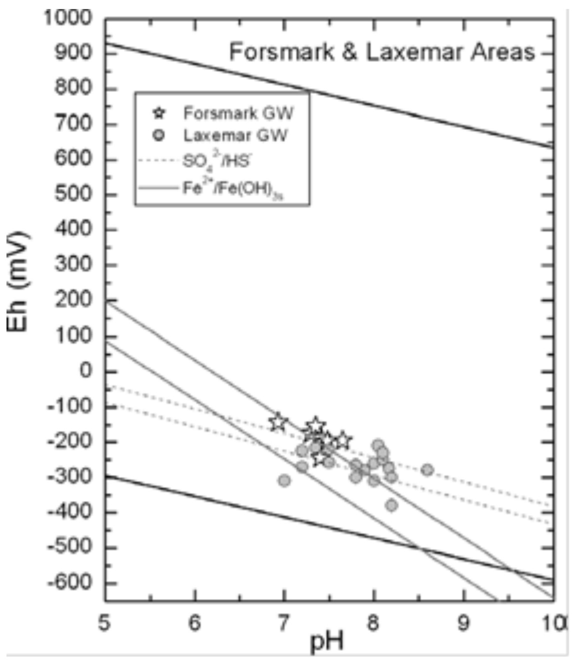

Figure A- 2. Eh and pH ranges at Swedish sites (Eh generally decreases with depth) (Laaksoharju et al., 2008).

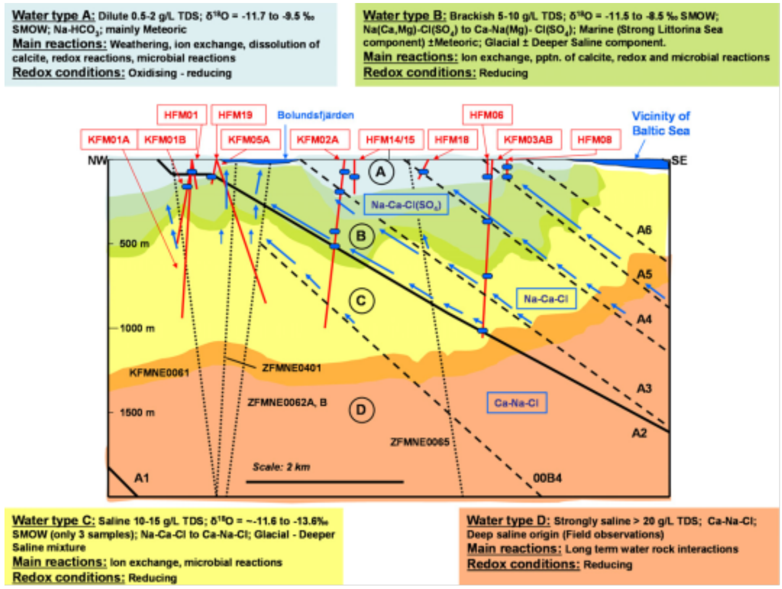

Forsmark site.

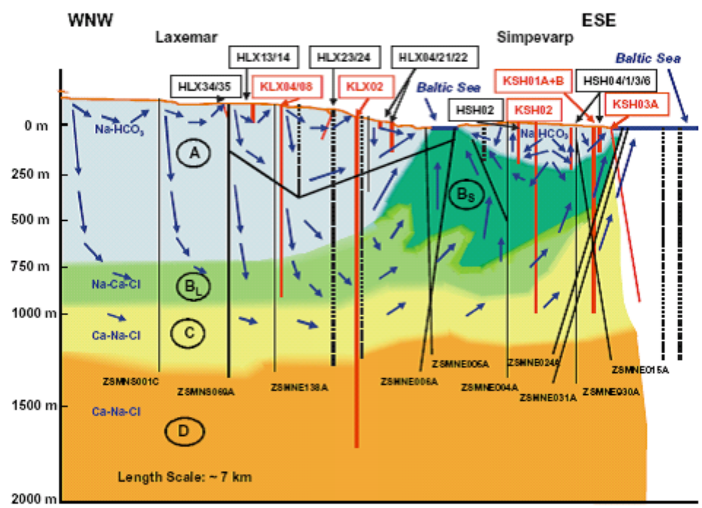

Laxemar/Simpevarp site

Figure A- 3. Types and distributions of groundwater at two Swedish granite sites (Laaksoharju et al., 2008).

A - fresh groundwater (<2000 mg/L Cl; 0.5–3.5 g/L TDS), mainly meteoric and Na–HCO3 in type, and marginally oxidizing close to the surface, otherwise reducing.

BL - brackish groundwater (2000–10,000 mg/L Cl; 3.5–18.5 g/L TDS), meteoric, mainly Na–Ca–Cl in type, glacial/deep saline components, and reducing.

BS - brackish groundwater (2000–10,000 mg/L Cl, 3.5–18.5 g/L TDS). meteoric, mainly Na–Ca–Cl in type but some Na–Ca(Mg)–Cl(Br) types, glacial/deep saline components, and reducing;

C -saline (10,000–20,000 mg/L Cl; 18.5–30 g/L TDS), dominantly Ca–Na–Cl in type at Laxemar but Na–Ca–Cl changing to Ca–Na–Cl only at the highest salinity levels at the Simpevarp site, and reducing.

D -highly saline (>20,000 mg/L Cl; to a maximum of ~70 g/L TDS), dominantly Ca–Na–Cl, and reducing.

Table A- 11. Groundwater chemistry of Switzerland Grimsel test site (~1730 m above sea level) (Schafer and Iijima, 2007). Low ionic strength water (~0.001 M, ~50 mg/L TDS), dominated by NaHCO3 (secondary ions are Ca2+ and Cl-) with Eh = -200 ± 50 mV and pH = 9.5 ± 0.2.

Parameter	Value	Unit
pH	9.6	
Eh	-170	mV
Ionic Strength	0.0017	M
Na	0.56	mM
K	0.006	mM
Mg	0.00058	mM
Ca	0.14	mM
Al	12.7	ppb
SO_4^{2-}	0.052	mM
F^-	0.31	mM
Cl^-	0.15	mM
HCO_3^-	0.283	mM

Appendix A References

Carbol, P. and I. Engkvist, 1997. Compilation of radionuclide sorption coefficients for performance assessment. SKB rapport R-97-13.

Gascoyne, M., 2004. Hydrogeochemistry, groundwater ages and sources of salts in a granitic batholith on the Canadian Shield, Southeastern Manitoba. Applied Geochemistry, Vol. 19, p519-560.

Iwatsuki et al., 2005. Hydrochemical baseline condition of groundwater at the Mizunami underground research laboratory (MIU). Applied Geochemistry, Vol. 20, p2283-2302.

JAEA (Japan Atomic Energy Agency), no date. Diffusion and sorption coefficient database. Japan Atomic Energy Agency. http://migrationdb.jaea.go.jp/english.html.

Kalinina et al., 2012. Analysis of the Effect of Heterogeneity on Heat Extraction in an EGS Represented with the Continuum Fracture Model. Proceedings of 37th Stanford Geothermal Reservoir Engineering Workshop, January 30 – February 1, 2012, Stanford, California.

Laaksoharju et al., 2008. Hydrogeochemical evaluation and modelling performed within the Swedish site investigation programme. Applied Geochemistry, Vol. 23, p1761-1795.

Mariner et al., 2011. Granite Disposal of U.S. High-Level Radioactive Waste. Sandia report SAND2011-6203, Sandia National Laboratories, Albuquerque, NM.

Painter et al., 2008. Time domain particle tracking methods for simulating transport with retention and first-order transformation. Water Resources Research 43(9), W01406.

Posiva, 2010. Models and Data Report 2010. POSIVA 2010-01. Posiva Oy, Olkiluoto, Finland.

Schafer, T. and K. Iijima, 2007. CFM Phase I – Status report of the laboratory programme. Nagra Report NAB 07-41, National Cooperative for the Disposal of Radioactive Waste, Wettingen, Switzerland.

SKB, 2006. Long-term Safety for KBS-3 Repositories at Forsmark and Laxemar — A First Evaluation. Technical Report TR-06-09. Swedish Nuclear Fuel and Waste Management Co.

SKB, 2010a. Radionuclide transport report for the safety assessment SR-Site. Technical Report TR-10-50. Swedish Nuclear Fuel and Waste Management Co.

SKB, 2010b. Data report for the safety assessment SR-Site. Technical Report TR-10-52. Swedish Nuclear Fuel and Waste Management Co.